RADIO SCIENCE Journal of Research NBS/USNC–URSI
Vol. 69D, No. 4, April 1965

High Frequency Backscatter From the Earth Measured at 1000 Km Altitude

R. C. Chia, A. K. Fung, and R. K. Moore

Center for Research in Engineering Science, University of Kansas, Lawrence, Kans.

(Received October 5, 1964)

Radar type backscatter from the ground to the Alouette satellite has been observed in the 9 megacycle frequency range. These are the first observations of the earth by radar from satellite altitudes.

Observations of effective reflection coefficients from the 1000 km altitude of the Alouette satellite have been made for 12 examples over the southern hemisphere, at frequencies in the order of 9 Mc/s. The absolute calculated ground effective reflection coefficient ranges from −24.1 dB for the forest to −5.4 dB for the sea. Relative values (ratio of ground to ionosphere effective reflection coefficients) range from 0.10 for the forest to 0.53 for the sea. Estimated variability of the data is ±3.6 dB. It is possible that the ground reflection coefficients are somewhat smaller than the correct value because attenuation in the ionosphere at 9 Mc/s has been neglected, and methods to correct for this are being studied.

1. Introduction

Radar type backscatter from the ground to the Alouette satellite has been observed in the 9 megacycle frequency range. These are the first observations of the earth by radar from satellite altitudes. Effective reflection coefficients are of the order expected by extrapolation of lower altitude measurements. Exact comparisons are difficult because of uncertainties about the data and difference in frequency between these and previous observations.

The Alouette satellite constructed by the Defense Research Board of Canada carries a topside ionosphere sounder sweeping in frequency from about 0.5 to 12 Mc/s. When the critical frequency of the ionosphere is less than 12 Mc/s, the transmitted signal penetrates the ionosphere and may be reflected or scattered back to the sounder as a ground echo. When the ionosphere is reasonably stable and the critical frequency is low enough, these ground echoes may be analyzed to determine effective reflection coefficients for that part of the earth over which the satellite is flying. The topside sounder, therefore, may be considered a downward-looking radar much like a radar altimeter. It obtains vertical incidence, relatively low frequency, radar measurements of the earth.

Radar observations of the earth from satellite altitudes are potentially valuable as a tool for studying the earth itself, as a technique for evaluating radar observations from the moon and planets and as an aid to the design of radar altimeters for rocket vehicles landing on the earth and planets. A similar technique may prove to be especially useful on spacecraft orbiting other planets. The low frequencies associated with the Alouette radar cause problems in the presence of an ionosphere such as that of the earth, but the problems will be reduced where the density of the ionosphere is less.

TABLE 1. *Previous near-vertical experiments*

Altitude	Experimenter	Frequency Range
Below 150 ft	Ohio State University	X and K band.
	NRL (Grant & Yaplee)	X, K, and Q band.
	Texas Instruments at Waterways Experiment Station	C, X, K_a band.
500 to 12,000 ft	TRE (England) (Clegg et al.)	X band.
	Davies & MacFarlane	X band.
	Sandia Corp.	400, 1,600, & 4,000 Mc/s.
	NRL (Katzin et al.)	400, 1,200, 3,000, & 9,000 Mc/s.
	General Precision Labs	X band.
Up to 67,000 ft	Auburn University	1,600 Mc/s.
Acoustic Simulation	University of New Mexico	

Previous measurements of radar reflection and scatter from the earth have been made at various altitudes and frequencies. Table 1 summarizes a number of these measurements, but is not intended to be an exhaustive summary. Only the Auburn University measurements were made at altitudes significantly above 12,000 ft, and this set of measurements was only made over water. The University of New Mexico acoustic simulations using nonlinear modeling were carried to equivalent altitudes of several hundred kilometers, but concentrated on the variation of the return with angle rather than its absolute magnitude.

Truly long distance backscatter measurements have been made only of lunar radar echoes. Many attempts have been made to describe a possible lunar surface based upon these echoes and other information available. Unfortunately, the extrapolation had to be carried all the way from the 12,000 ft altitudes of aircraft experiments to the lunar distances so that the disagreement as to interpretation among various writers is not surprising. With the successful Ranger photographs of the lunar surface, some of the argu-

ments about this interpretation may decrease, but the same problem arises in interpreting echoes from other planets. The various theories are neither precise enough nor sufficiently agreed upon that they can predict, with accuracy, the type of signal likely to be observed by a satellite radar at a particular frequency—at least not without some experimental confirmation. This study represents the first attempt at such a confirmation.

2. Alouette as a Backscatter Radar

The Alouette satellite was launched on September 29, 1962, into an orbit inclined at an angle of 80.46 deg by the U.S. National Aeronautics and Space Administration. The experiment package was constructed by the Defense Research Telecommunications Establishment of the Defense Research Board of Canada. The ionosphere topside sounder was the principal experiment, although three other experiments were also a part of the system. Characteristics of the sounder are shown in table 2 [Franklin et al., 1963].

TABLE 2. *Alouette sounder system parameters*

System	Parameter	Remark
T_r	Frequency sweep	0.45 to 11.8 Mc/s in approx. 12 sec.
	Pulse width	100 μ sec.
	Pulse repetition frequency	67 pps.
	Peak pulse power	Approx. 100 W into 400 ohm load.
R_r	Frequency sweep	0.45 to 11.8 Mc/s.
	Noise figure	8 dB.
	Minimum signal detection through antenna matching networks	19 dB above kTB.
Antenna	Dipole 1	150 ft tip to tip for 0.45–4.8 Mc/s.
	Dipole 2	75 ft tip to tip for 4.8–11.8 Mc/s.

The upper frequency limit of the sounder is lower than one would prefer for ground echo studies, but certainly is high enough for its intended purpose of ionosphere sounding at this time of the sun spot cycle. Because of a large number of interfering signals in the top 2 Mc/s of the sweep range, it was decided to concentrate on the frequency range from 9 to 10 Mc/s for ground echo studies. Successive pulses are separated in carrier frequency by about 15 kc/s so that the number of pulses in the usable range is at most about 70.

With the 100 μsec pulse and the 1000 km orbit, the first pulse length on the ground illuminates a circle with radius 173 km, corresponding to an illuminated cone with an apex angle of 20 deg. Because of this large angle and the relatively weak signals, it is not possible to get much information from the shape of the received pulse about the variation of scattering as a function of angle.

The dipole antenna on the satellite has a broad pattern and the satellite axis is inclined with respect to the radial direction by a maximum of around 20 deg. Consequently, no significant correction in the returns is required because of antenna tilt. It is assumed here that the antenna pattern is the same as it would be if the antenna were in space. Rocket experiments indicate that the major effects on antenna impedance, at least, are over by the time the rocket reaches the orbital altitude of the Alouette [Crouse et al., 1964], so it is believed that this is a safe assumption.

In many locations the ground signal is too weak to be measured accurately. This is due in part to the scattering properties of the ground, in part to the ionosphere, and in large part to the presence of many interfering signals at various frequencies within the range of interest. Interfering signals are particularly bad in the northern hemisphere. Consequently, it has been found desirable to select southern hemisphere stations for most of the analysis. At these stations, the signal-to-noise ratio appears reasonable for a majority of the pulses within the frequency range of interest, whereas in the northern hemisphere it is often reasonable only for a few pulses in the appropriate range.

The ionospheric conditions at a particular time determine whether the ground signal at that time can be used. At times the critical frequency of the ionosphere is about 10 Mc/s. Obviously no ground echoes are available then. Ordinarily ground echoes are selected for observation only when the critical frequency is at or below 7 Mc/s. There may be significant attenuation in the F layer during the daytime, even at frequencies a quarter to a third higher than the critical frequency.

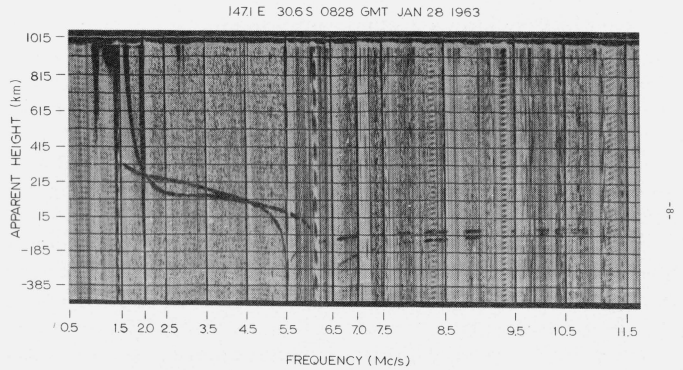

FIGURE 1. *Usable ground echo.*

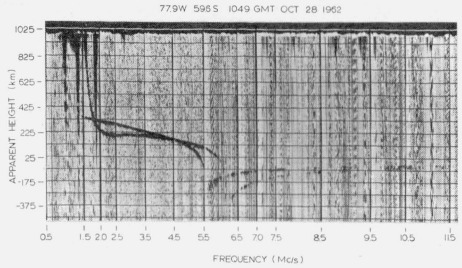

FIGURE 2. *Unusable ground echo.*

Turbulence in the ionosphere is a basis for excluding from consideration ground echoes from a particular sweep. In the polar regions such turbulence is nearly always present so that observations studied here are primarily limited to temperate and tropical regions. Figures 1 and 2 show ionograms associated with usable and unusable ground echoes, respectively.

Transmission through the ionosphere causes magneto-ionic splitting of the waves. This splitting is observable on the ground echoes. When the critical frequency is low enough, the ordinary and extraordinary ground echoes are merged in the frequency range of interest. Many times, however, they are separate and easily identifiable. Occasionally, four traces are observed representing further splitting of each of the ground reflected waves. Sweeps where these four traces are all visible have not been used in the analysis.

The satellite receiver has a strong automatic gain control set either by cosmic noise or by interfering signals. The level of the AGC voltage is telemetered to the ground, but errors are introduced because the receiver sensitivity varies so greatly for such small changes in AGC level.

3. Effective Reflection Coefficient

Radar observations at wavelengths of slightly under a meter have indicated that surfaces smooth to this order are very difficult to find in nature. [Edison et al., 1960 and Taylor, 1959]. Various theories indicate that a surface is smooth enough to give specular reflection only if the mean square fluctuation about the mean height is less than about a tenth wavelength. [Moore, 1957 and Hayre, 1962]. Over the sea, this condition may frequently be met at the wavelength of about 30 m involved in this experiment. It is unlikely that land surfaces will be this smooth over a distance as great as that indicated by the diameter (347 km) of the illuminated circle directly beneath the satellite. Consequently, it is to be expected that land echoes will be primarily due to scattering rather than Fresnel reflection, and also sea echoes may often be scattered.

The power received from a rough scattering surface is expressed by

$$W_r = \int_{\substack{\text{Illuminated}\\ \text{Area}}} \frac{W_t \lambda^2 G^2}{(4\pi)^3 R^4} \sigma_0 \, dA \tag{1}$$

where W_t = Transmitted power
G = Antenna gain
R = Distance from the transmitter to a point in the illuminated area
σ_0 = Scattering cross section per unit area
A = Illuminated area
λ = Wavelength.

For pulse-length limitation of the illuminated area on the ground with rectangular pulses and essentially constant antenna gain, this integral reduces for the "altitude signal" to

$$W_r = \frac{W_t \lambda^2 G^2}{2(4\pi)^2} \int_h^{h+\frac{c\tau}{2}} \frac{\sigma_0 dR}{R^3} \tag{2}$$

where h = Altitude
c = Velocity of light.
τ = Pulse length.

We may express this integral in terms of the angle rather than the range in which case it is

$$W_r = \frac{W_t \lambda^2 G^2}{2(4\pi)^2 h^2} \int_0^{\tan^{-1}\frac{c\tau}{h}} \sigma_0(\theta) \sin\theta \cos\theta d\theta \tag{3}$$

where θ is the angle made by an element on the ground with the vertical.

Experiment and theory both indicate that for surfaces that are relatively smooth with respect to a wavelength, σ_0 decreases rapidly with increasing θ in the vicinity of the vertical. It is likely that most grounds (at least outside of mountain areas) will satisfy this criterion for 30 m wavelengths. Consequently, most of the contribution to the integral normally comes from angles considerably under 10 deg. This means

$$\sigma_0\left(\tan^{-1}\sqrt{\frac{c\tau}{h}}\right) \ll \sigma_0(0). \tag{4}$$

When this situation prevails, the upper limit determined by pulse length is immaterial. That is, the radiation is essentially limited by the beam angle of the backscattering rather than by the pulse length. When this is true an arbitrary upper limit such as $\frac{\pi}{2}$ may be placed on the integral without significant error:

$$W_r \approx \frac{W_t \lambda^2 G^2}{(4\pi)^2 (2h)^2} \int_0^{\frac{\pi}{2}} \sigma_0(\theta) \sin 2\theta d\theta. \tag{5}$$

This equation is the same as that for a specular reflection where the integral is the square of the Fresnel

reflection coefficient. Thus, we may define

$$K_{\text{eff}}^2 = \int_0^{\frac{\pi}{2}} \sigma_0(\theta) \sin 2\theta d\theta \qquad (6)$$

as the square of the effective Fresnel reflection coefficient, K_{eff}.

Beam-width-limited illumination is characterized by the expression

$$W_r = \left[\frac{W_t \lambda^2 G^2}{(4\pi)^2 (2h)^2}\right] \int_0^{\theta_0} \sigma_0(\theta) \sin 2\theta d\theta \qquad (7)$$

where θ_0 is the limit of the beam, in which the variation with height is the same as that for a specular reflection. Pulse-length limitation, on the other hand, corresponds to a different variation with height. [Moore et al., 1957.] Thus, use of this effective reflection coefficient implies beam-width limitations. In this case, the beam is set by the scattering coefficient rather than by the width of the antenna patterr as it is in some microwave vertical-looking radars.

The use of the effective reflection coefficient may or may not imply that Fresnel reflection does, in fact, occur. If Fresnel reflection occurs, the signal should not fade in amplitude. If scattering occurs, the signal should fade, as contributions from the different scatterers add successively in and out of phase.

4. Data Analysis

Figure 3 shows a simplified block diagram of the sounder. Computation of system sensitivity can be understood better by referring to this diagram. Unfortunately the calibrations had to be obtained on the ground somewhat piecemeal because the antennas were not self supporting in the presence of gravity.

Transmitter power was measured at various frequencies in a dummy antenna. Receiver output, as a function of input at the junction of the transmitter and TR switch lines, was measured at various frequencies. Based on the calculated impedance of the antenna and the properties of the matching network, it was then possible to calculate the power received at the antenna for a given receiver output. There are, of course, uncertainties associated with such calculations which could be resolved if the antenna could be measured extended, but this was not possible.

Variations in the performance of the telemetry link do not effect the result, because a "line sync unit" is the standard amplitude measure. This is determined by a calibration pulse transmitted once for each transmitter pulse which accurately determines the transfer gain for the telemetry, recording, and play-back system.

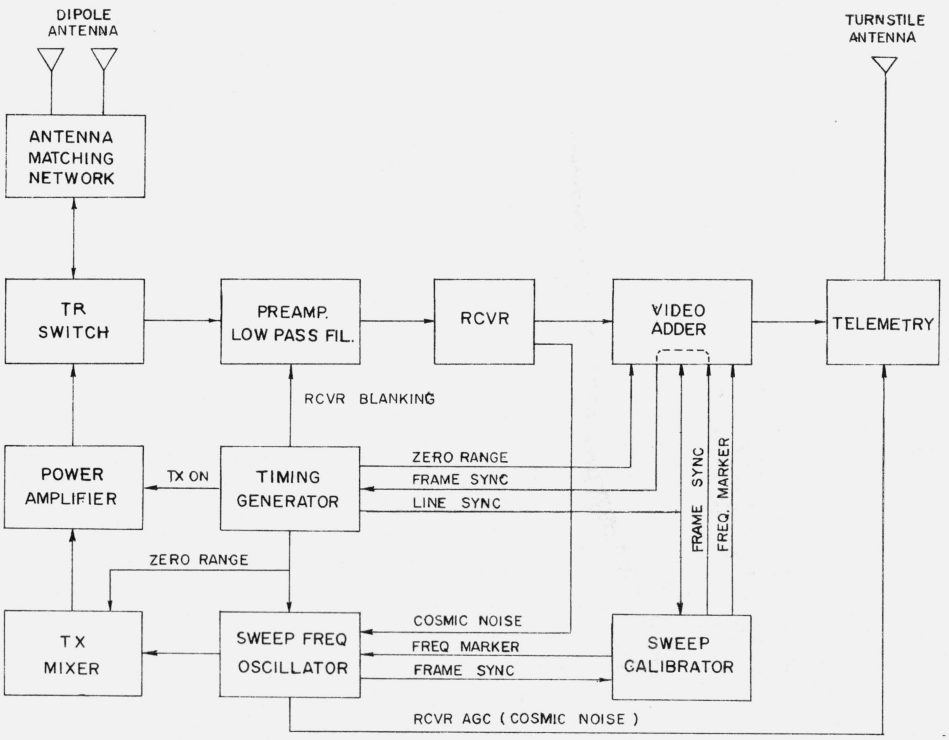

FIGURE 3. *Simplified block diagram of the sounder.*

Table 3 illustrates the anticipated errors in the various quantities for both ionosphere and ground echoes. Maximum overall RMS error has been obtained from these. It is ±3.60 dB.

TABLE 3. *Summary of errors.*

Parameter	Variation range	Selected reference	Max. error in dB
Signal reading	±4 percent		
Line Sync reading	±3 percent		
AGC reading	±1 percent		
AGC input curves			±1.50
Reading errors			±2.00
Antenna gain		1.31	±1.50
For lower frequency:			
Frequency	4.9–5.5 Mc/s	5.2 Mc/s	±0.25
Transmitted power	7–9 dB below 100 W	7 dB below 100 W	±1.20
Altitude	600–800 km	700 km	±1.00
RCVR input Z_R		366–j99 ohm	±1.00
Mismatch loss		2.86 dB	±1.00
For higher frequency:			
Frequency	8.7–9.3 Mc/s	9.0 Mc/s	±0.15
Transmitted power	6.6–8.2 dB below 100 W	7 dB below 100 W	±1.20
Altitude	1004–1050 km	1000 km	−0.20
RCVR input Z_R		311–j66 ohm	±1.00
Mismatch loss		1.7 dB	±0.50
Maximum possible overall RMS error			±3.60

Because of the usual difficulties associated with absolute signal measurements, a relative procedure to obtain ground effective reflection coefficients in terms of ionosphere reflection coefficients was devised. The results are presented side by side so the reader may draw his own conclusions. It is assumed that the reflection coefficient of the ionosphere is unity, and that no attenuation occurs from the satellite down to the level of reflection. With these assumptions, the effective reflection coefficient of the ground is simply the ratio of the corrected transmission ratios $\left(\frac{W_r}{W_t}\right)$ for the ground and ionosphere echoes. This technique may introduce as many errors as it removes because the ionosphere echo must, of course, be at a different frequency than the ground echo. Because of possible attenuation at lower frequencies and because use of the same antenna for both ionosphere and ground echoes seems desirable, a frequency range for ionosphere echoes of 4.9 to 5.5 Mc/s was selected. A fixed distance to the ionosphere was assumed (700 km) and the records were not, in fact, scaled for the correct distance, this procedure does not introduce as much uncertainty as other possible errors. This is indicated in table 3. The transmitter power output is different at the different frequencies as is the receiver mismatch loss and the antenna gain. All of these factors have been taken into account in computation of the relative reflection coefficient. Since the antenna characteristics are changing more rapidly near 5 Mc/s than near 9 Mc/s, the ionosphere echo calibration may actually be in more doubt than the ground echo calibration. On the other hand, any systematic large error that is relatively independent of frequency is readily removed by use of this technique. Furthermore, a fluctuation of a reflection coefficient measured for the ionosphere gives an indication of the accuracy with which the absolute calibration can be counted upon.

More details of the data handling procedure are given in appendix A.

5. Experimental Results

Table 4 shows the effective reflection coefficients calculated for several different terrains on both the absolute and relative basis. Effective reflection coefficients of the ground are, in general, about as expected. The variability of reflection coefficients of the ionosphere is of the same order as predicted in table 4. The mean value of these measurements is 0.895 indicating that systematic errors appear small near 5 Mc/s.

Figure 4 and table 5 show the locations of the various areas considered. The descriptions of the targets were obtained from examination of detailed vegetation maps of the areas involved. As yet no attempt has been made to determine the state of the sea in the two ocean areas so that this may be correlated with the echo strength.

Table 6 compares the results obtained in this fashion with comparable data from other observers at other frequencies.

TABLE 4. *Effective reflection coefficient from several different terrains.*

Terrain	Location	Effective reflection coefficient			Local time
		Absolute		Relative	
		Ionosphere K_i	Ground K_g	K_g/K_i	
Ocean	South Atlantic	1.019	0.54	0.530	0559 Oct 27 '62
Ocean	South Pacific	1.368	0.324	0.237	1803 Jan 28 '63
Forest	Australia	0.652	0.062	0.095	1808 Jan 28 '63
Tropical woodland	Australia	0.520	0.137	0.264	1817 Jan 28 '63
Tropical woodland	Australia	0.946	0.228	0.241	1817 Jan 28 '63
Tropical woodland	Australia	0.892	0.377	0.422	1819 Jan 28 '63
Forest scrub	Australia	1.013	0.203	0.200	0706 Jan 28 '63
Forest scrub	Australia	0.673	0.256	0.380	0706 Jan 28 '63
Low shrub woodland	Australia	0.516	0.178	0.345	0712 Jan 28 '63
Sand	Australia	0.703	0.206	0.293	0741 Jan 22 '63
Sand	Australia	0.998	0.388	0.389	0747 Jan 22 '63
Stony desert	Australia	0.956	0.172	0.180	0749 Jan 22 '63

FIGURE 4. *Sampled terrains over Australia.*

TABLE 5. *Geographical locations of the sampled terrains.*

Target No.*	Long. (E)	Lat. (S)	Terrain
1	144.6°	43.5°	Ocean
2	145.5°	41.0°	Forest
3	147.1°	30.6°	Tropical woodland
4	147.3°	29.6°	Tropical woodland
5	147.7°	27.6°	Tropical woodland
6	146.4°	30.8°	Forest scrub
7	146.6°	31.5°	Forest scrub
8	148.0°	39.5°	Low shrub woodland
9	133.2°	16.3°	Sand
10	134.2°	24.7°	Sand
11	134.4°	26.3°	Stony desert

*See figure 4.

TABLE 6. *Power reflection coefficients at several different frequencies.*

Observer	Frequency	Altitude	Terrain			
			Forest	Desert	Sand	Water
Sandia[c] Corp.	415 Mc/s	12000 ft	−12 to −21 dB	−13 dB		−1[b] dB
		8000 ft			−6 dB	
		7000 ft				+1[a] dB
	3800 Mc/s	12000 ft	−13 to −16 dB	−14 dB		+2[b] dB
		7000 ft				+1[a] dB
Auburn[d] University	1600 Mc/s	2000 to 70000 ft				−3[a] to −5[b] dB
Alouette	9 Mc/s	1000 km	−8.5 to −24 dB	−8 to −15 dB		−5 to −10 dB

[a] Smooth water.
[b] Rough water.
[c] Edison et al., 1960.
[d] Summer, 1963.

6. Conclusions

Observations of effective reflection coefficients from the 1000 km altitude of the Alouette satellite have been made for 12 examples of the earth surface, at frequencies in the order of 9 Mc/s. The absolute calculated ground effective reflection coefficient ranges from −24.1 dB for the forest to −5.4 dB for the sea. Relative values range from 0.10 for the forest to 0.53 for the sea. Estimated variability of the data is ±3.6 dB. It is possible that the ground reflection coefficients are somewhat smaller than the correct value because attenuation in the ionosphere at 9 Mc/s has been neglected, and methods to correct for this are being studied.

The authors thank Dr. E. S. Warren and the staff of the Defense Research Telecommunications Establishment, Ottawa, Canada, for supplying the information required in this work, which is supported by the National Aeronautics and Space Administration under research contract NsG 477.

7. Appendix A. Data Handling Procedure

Alouette satellite video signals are recorded on magnetic tape. AGC signals are recorded on another channel of the tape. For this type of analysis, the taped signals are recorded on film on a pulse-by-pulse basis by displaying them on an oscilloscope and using

a camera with a fast moving 35 mm film. Figure 5 shows a typical trace as recorded on film. The baseline is not horizontal because of the relative speeds of film motion and oscilloscope beam.

Figure 6 shows a simplified sketch indicating the characteristics of the pulse as seen on the film. The basic unit for all observations is the line sync unit. In order to determine the line sync unit and the pulse height it is necessary to locate the correct zero level. Immediately following the zero range pulse is a period during which the receiver is inactive. This pulse is used in establishing the zero level. It is offset from the actual zero by a calibrated amount which is a function of the AGC voltage, and was measured prior to flight.

Frequency markers are inserted in the record at the intervals shown on figure 7 and can be readily identified on the pulse-to-pulse photos. Records are selected for analysis by observation of the ionograms to determine suitability both in terms of a stable ionosphere and suitable ground echoes sufficiently far removed from the critical frequency.

The AGC signal is correlated with the appropriate trace by use of a dual beam oscilloscope one beam being assigned to the video and the other to the AGC signal. Zero level for the AGC is determined during the frequency marker interval and the AGC is calibrated with a stair-step voltage provided once for each pass. To aid in establishing these levels a film is first exposed with identical oscilloscope and recorder settings, but with film motion at right angles to that used on the pulse-by-pulse recording. (See fig. 7.)

In practice, AGC for a particular pulse is determined by reading the spacing between the baseline of the video (AGC reference) and the AGC line. Signal return and line sync are measured relative to the offset zero level immediately following zero range pulse and corrections are made for the d-c offset later in the process of analysis.

A typical calculation to indicate the procedure followed after the AGC voltage and signal level in line sync units have been determined as follows:

For a typical pass over the South Atlantic Ocean, primary readings in mm taken from the microfilm reader are listed in columns A, B, and C of table 7.

AGC voltage values given in column D are converted from the readings in column C. For this particular pass, the AGC reference has a reading of 43 mm and the AGC calibration value is given as every 11 mm reading corresponding to 1.25 V. Thus, for instance, the AGC listed for frame No. 29 is obtained from the relation

$$(62-43)\times\frac{1.25}{11}=2.16 \text{ V.}$$

The d-c offsets in column E are given in line sync units. Once the AGC value is known, the d-c offset can be read directly from figure 8.

Column F gives the true length of the line sync for each individual frame by taking the d-c offset into consideration.

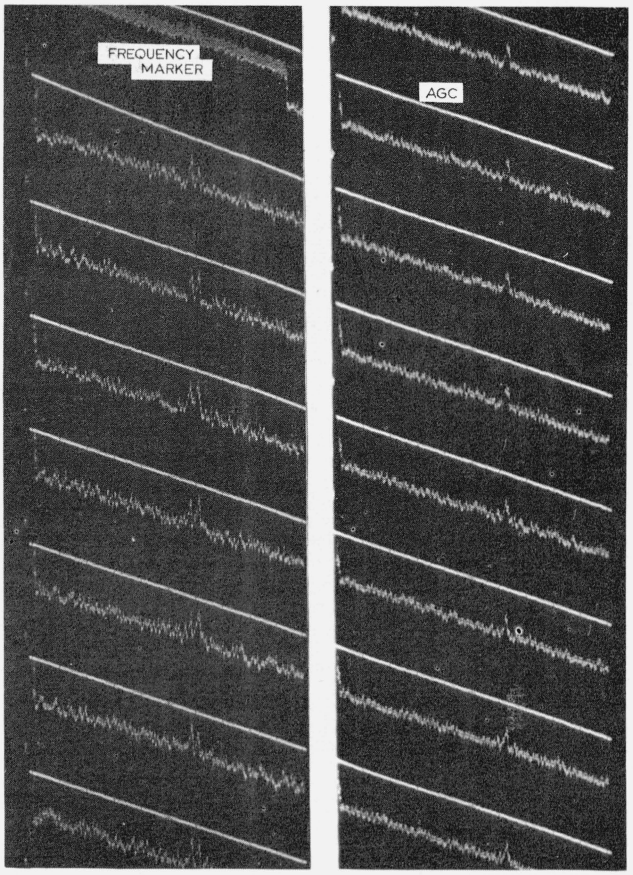

FIGURE 5. *Typical traces on film.*

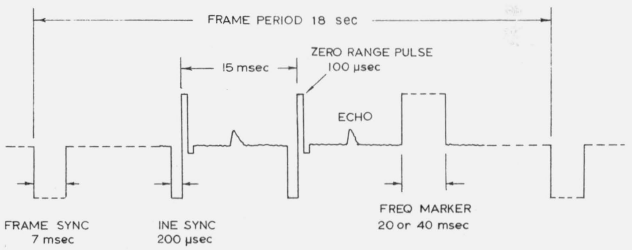

FIGURE 6. *Video signal for ionospheric data link.*

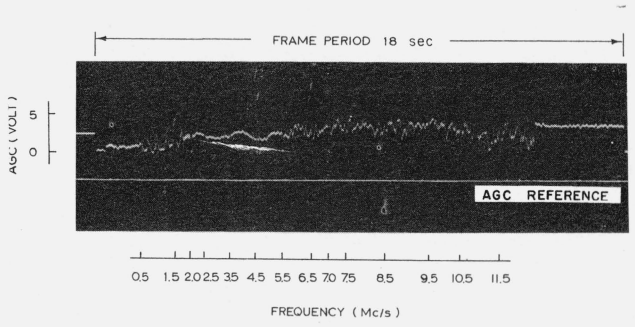

FIGURE 7. *Frequency markers and AGC.*

TABLE 7. *Data processing chart.*

Frame No.	Reading (mm)			Conversion					Results	
	A	B	C	E	F	G	H	D	$I_{(\mu V)}$	J
	Line sync	Signal	AGC	D-C offset	A/(1+E)	B/F	G+E	AGC (V)	Signal	I^2
29	58	36	62	0.064	54.5	0.66	0.72	2.16	49.5	2450
30	56	34	61	.061	52.8	.64	.70	2.04	38.0	1440
31	56	34	61	.061	52.8	.64	.70	2.04	38.0	1440
32	56	32	62	.064	52.6	.61	.67	2.16	31.5	990
33	58	36	62	.064	54.5	.66	.72	2.16	49.5	2450
34	58	36	62	.064	54.5	.66	.72	2.16	49.5	2450
35	54	32	65	.070	50.5	.63	.70	2.50	54.5	2970
36	54	32	64	.068	50.6	.63	.70	2.39	49.0	2400
37	54	30	63	.066	50.6	.59	.66	2.27	31.0	960
38	56	32	60	.058	52.9	.60	.66	1.93	25.0	630
39	56	32	60	.058	52.9	.60	.66	1.93	25.0	630
40	56	34	61	.061	52.8	.64	.70	2.04	38.0	1440
41	58	36	62	.064	54.5	.66	.72	2.16	49.5	2450
42	58	36	62	.064	54.5	.66	.72	2.16	49.5	2450
43	58	34	63	.066	52.5	.65	.72	2.27	53.3	2860
44	58	32	62	.064	52.6	.61	.67	2.16	31.5	990
45	54	32	62	.064	50.8	.63	.69	2.16	38.0	1440
46	56	34	63	.066	52.5	.65	.72	2.27	53.3	2860
47	54	34	62	.064	50.8	.67	.73	2.16	53.0	2810
48	56	36	61	.061	52.8	.68	.74	2.04	50.5	2550

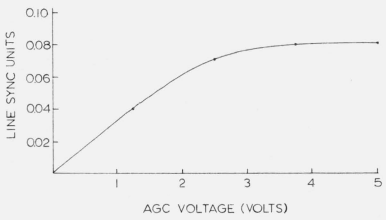

FIGURE 8. *Zero d-c offset versus AGC voltage.*

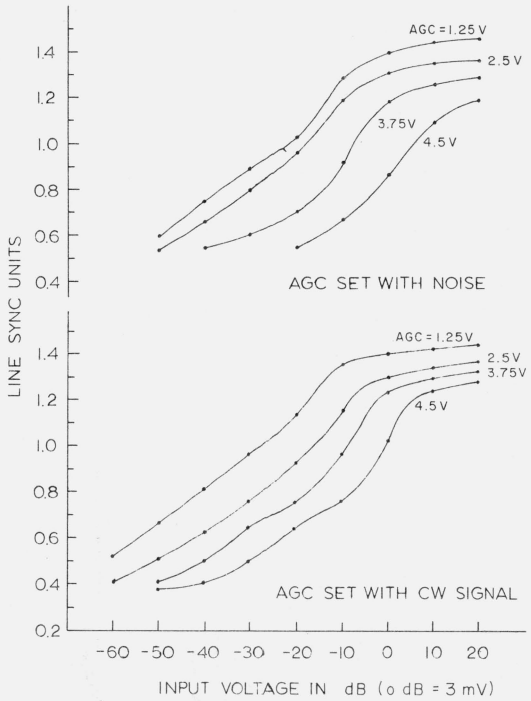

FIGURE 9. *Input voltage versus AGC at 9 Mc/s.*

Column G is the apparent signal height in line sync units, while column H gives the true signal level in line sync units.

From the AGC curves given at 9 Mc/s (fig. 9), voltages at the receiver input terminals can be deduced by interpolating linearly between curves according to the given signal levels in line sync units (column H) and the AGC voltages (column D). The input voltage readings in microvolts are listed in column I and their square values in column J.

For these 20 sampling data, the mean square value of the input voltage is found to be

$$\overline{V}_R^2 = 1930 \times 10^{-12}(\mathrm{V})^2.$$

An approximate 95% confidence interval is constructed by checking with the sampling variance, S. For this example $S = 815$. No sample value is greater or less than $\overline{V}_R^2 \pm 2S$, i.e., $300 < V_R^2 < 3560$. Thus, $\overline{V}_R^2$ is a reasonably safe estimate.

Assuming the transmitted power is evenly distributed over the ordinary and the extraordinary waves in the ionosphere, the calculated voltage square value is raised by 3 dB in order to take care of the ionospheric splitting. Thus, the mean square value of the input voltage at the receiver is modified to

$$V_R^2 = 3860 \times 10^{-12}(\mathrm{V})^2.$$

Receiver input impedance from the DRTE-supplied table, averaged around 9 Mc/s, is

$$Z_R = 311 - \mathrm{J}66 \text{ ohms}.$$

Mismatch loss (from given curves) at 9 Mc/s is

$$L_m = 1.7 \text{ dB}.$$

Power into the receiver, W'_R, is calculated as

$$W'_R = V_R^2 \frac{R_R}{Z_R Z_R^*} = 11.91 \times 10^{-12} \text{W}.$$

By taking the mismatch loss into account, the power received at the antenna is then corrected to

$$W_R = 11.91 \times 10^{-12} \times 10^{0.17} = 17.62 \times 10^{-12} \text{ W}.$$

From the curve, which shows frequency versus transmitter output into simulated antenna impedance, the transmitted power at 9 Mc/s is

$$W_T = 20 \text{ W}.$$

The ground effective reflection coefficient K_g can thus be calculated from

$$K^2 = \frac{W_R (4\pi)^2 (2h)^2}{W_T G^2 \lambda^2} = 0.291.$$

Hence $K_g = 0.54$ (absolute).
The other constants in the above calculation are chosen as:

Satellite altitude $h = 10^6$ m above ground;
Antenna gain for a conventional dipole antenna $G^2 = 1.72$;
Wavelength at 9 Mc/s $\lambda = \frac{1}{3} \times 10^2$ m.

By a similar process, the effective reflection coefficient for ionosphere over the same target at 5.2 Mc/s is obtained as

$$K_i = 1.019 \text{ (absolute)}.$$

Hence, the relative ground effective reflection coefficient for the ocean at this point is

$$\frac{K_g}{K_i} = 0.53.$$

8. References

Crouse, P. E., Nisbet, J. S., and T. A. Seliga (April 1964), Electron densities and collision frequencies from low frequency probe measurements, presented at the Spring URSI–IEEE Meeting, Washington, D.C.

Edison, A. R., Moore, R. K., and B. D. Warner (May 1960), Radar terrain return measured at near-vertical incidence, IRE Trans. Ant. Prop. **8**, No. 3, 246–254.

Franklin, C. A., Bibby, R. J., Sturrock, R. F., and D. F. Page (1963), Electronic and system design of the Canadian ionospheric satellite, IEEE Internat. Convention Record (USA) 11, part 5, 64–72.

Hayre, H. S. (1962), Radar backscatter theories for near-vertical incidence and their application to an estimate of the lunar surface roughness, Univ. of New Mex. Doctoral dissertation, 103.

Moore, R. K. (July 1957), Resolution of vertical incidence radar return into specular components, Univ. of New Mex., Engr. Expt. Sta. Tech. Rpt., EE–6.

Moore, R. K., and C. S. Williams, Jr. (1957), Radar terrain return at near-vertical incidence, Proc. IRE **45**, No. 2, 228–238.

Summer, H. M. (March 1963), A study of the radar reflectivity of sea water at vertical incidence, Auburn University, Tech. Report Contract NAS 8–2520.

Taylor, R. C. (1959), Terrain return measurement at X, K_u, and K_a band, IRE Nat. Conv. Record 7, Part 1, 19–26.

(Paper 69D4–499)